# Structural phase transition and magnetic anisotropy of La-substituted *M*-type Sr hexaferrite

Michaela Küpferling,* Roland Grössinger, Martin W. Pieper, Günter Wiesinger, and Herwig Michor
*Department of Solid State Physics, Vienna University of Technology, A-1040 Vienna, Austria*

Clemens Ritter
*Institute Laue-Langevin, F-38042 Grenoble, France*

Frank Kubel
*Department of Chemical Technologies and Analytics, Vienna University of Technology, A-1060 Vienna, Austria*
(Received 23 December 2005; published 7 April 2006)

La-substituted Sr hexaferrite with different La concentrations $x$ were prepared and investigated in order to observe changes in magnetic and structural properties with the substitution. With diffraction methods a change in crystal structure below approximately 100 K from hexagonal with spacegroup $P6_3/mmc$ to orthorhombic with spacegroup *Cmcm* was observed for the fully substituted La hexaferrite and attributed to a lattice distortion. A large increase in magnetocrystalline anisotropy of $LaFe_{12}O_{19}$ at low temperatures was confirmed by measurements and associated with the formation of an orbital momentum of $Fe^{2+}$ together with the lattice distortion. The localization of the $Fe^{2+}$ ion at the 2*a* site was determined from the Mössbauer spectrum, showing also an indication for an orbital momentum in the hyperfine field. In contrast, neither a structural phase transition nor the formation of $Fe^{2+}$ was observed at $x<1$ in x-ray diffraction or NMR spectroscopy.

DOI: 10.1103/PhysRevB.73.144408 PACS number(s): 75.50.Bb, 75.30.Gw, 61.66.Fn, 64.70.Kb

## I. INTRODUCTION

*M*-type hexaferrites were discovered in the 1950's in the research laboratories of Philips.[1] Due to the fact that they are ferrimagnetic their magnetization is comparably low and also the maximum achievable coercivity is ten times lower than the one of the rare earth compounds. Nevertheless hexaferrites are still covering more than 50% of the permanent magnet market. The main reasons are the low costs and the chemical stability of ferrites in contrast to rare earth compounds.

Because of their technical importance any improvement of the properties of the *M*-type ferrites is of relevance for the large market. Therefore, many attempts have been made to improve their magnetic properties by doping and substitutions within the complex structure, for the Ba or Sr ion as well as for the Fe ions. However, most types of substitutions investigated up to now, such as, e.g., Fe by Al, or Co and Ti, either cause a decrease of the saturation magnetization, or a drastic reduction of the magnetocrystalline anisotropy (for a survey see Ref. 2). Since the coercivity is determined mainly by magnetocrystalline anisotropy this also leads to a decrease of coercivity and, therefore, a reduction of the energy product of the permanent magnet. However, a very early work showing improved hard magnetic properties in samples doped simultaneously with La and Co went unnoticed,[3] so it came as surprise when the significant increase in room temperature coercivity upon La-Co substitution was rediscovered,[4] causing a remarkable comeback of research activities in substituted ferrites. The research included investigations of rare earth substituted hexaferrites,[5–7] which are interesting also due to a possible contribution of the magnetic moment of the rare earth element, most likely at low temperatures. Among the rare earth substitutions the complete substitution of Sr or Ba by La was promising, despite the missing magnetic moment, due to a very high anisotropy at low temperatures of this compound reported already in 1974 by Lotgering.[8] Nevertheless, only few investigations of this compound were performed, probably due to difficulties in preparation caused by the metastability of La hexaferrite.

The work presented here was started in order to clarify the role of the rare earth element in substituted *M*-type hexaferrites in enhancing magnetocrystalline anisotropy. For this reason La hexaferrite and La-substituted Sr hexaferrite with various La concentrations was prepared in order to explain how the properties of *M*-type hexaferrites change with the rare earth substitution of the Sr ion, and if an improvement with respect to the parent compound is possible. Different preparation methods were used and compared. In order to observe the change in magnetic and structural properties, the samples were examined by x-ray and neutron diffraction as well as nuclear magnetic resonance and Mössbauer spectroscopy, together with measurements of temperature dependent anisotropy and the low temperature hysteresis loop.

## II. EXPERIMENTAL

### A. Preparation of the samples

Four different methods were used, all typical for preparation of hexaferrites: mechanical alloying, as ceramic route, and three chemical methods, coprecipitation and two sol gel methods. For all methods it was possible to obtain the hexaferrite phase.[9] It was found that for the formation of this phase the main preparation steps are to perform a heat treatment within the temperature range of stability of this phase followed by a very rapid quenching. The reason is that La hexaferrite is a high temperature phase, which is metastable at room temperature and decomposes easily.[10] It was decided to concentrate on coprecipitation and mechanical alloying,

 

TABLE I. La-substituted Sr hexaferrites with nominal formula unit; the La excess used for the La hexaferrite and the amount of secondary phases is given.

| formula unit | method | La exc. [%] | sec. ph.[a] [w.t %] |
|---|---|---|---|
| $LaFe_{12}O_{19}$ | co.[b] | 50 | 10 |
| $LaFe_{12}O_{19}$ | MA[c] | 2 | 0 |
| $Sr_{0.66}La_{0.33}Fe_{12}O_{19}$ | co. | | 20 |
| $Sr_{0.88}La_{0.11}Fe_{12}O_{19}$ | MA | | 0 |
| $Sr_{0.8}La_{0.2}Fe_{12}O_{19}$ | MA | | 0 |
| $Sr_{0.66}La_{0.33}Fe_{12}O_{19}$ | MA | | 8 |
| $Sr_{0.5}La_{0.5}Fe_{12}O_{19}$ | MA | | 6 |
| $Sr_{0.25}La_{0.75}Fe_{12}O_{19}$ | MA | | 12 |
| $SrFe_{12}O_{19}$ | MA | | 0 |

[a]Secondary phases determined by XRD.
[b]Coprecipitation.
[c]Mechanical alloying.

which are common in ferrite production and more simple to perform than the sol gel methods.

For mechanical alloying[11] the starting materials were $La_2O_3$ and $Fe_2O_3$ in a ratio of 1/12. Different amounts of La excess in mol% were used in order to compensate for Fe excess due to milling in a steel vial. The mechanical alloying was done in a hardened steel vial together with 12 mm steel balls for 24 h using a Spex 8000 mixer/mill. The ball to powder mass ratio was 8:1.

For coprecipitation the starting materials were $La(NO_3)_3$ and $Fe(NO_3)_3$ in a ratio of 1/12 with various La excess, since some La loss is expected due to different solubility of the $La(OH)_3$ and the $Fe(OH)_3$. These were dissolved in a solution of water and ammonia, followed by a digestion step at 80 °C. This reaction results in a fine distribution of La and Fe hydroxides. The powder has been carefully washed, filtered and overnight dried prior to its oxidation at 800 °C for 24 h.

All samples were pressed with 3 bar, heat treated at temperatures around 1350 °C according to the furnace for approximately 24 h and subsequently quenched in water. In order to reduce the amount of secondary phases [$LaFeO_3$ (La orthoferrite) and $Fe_2O_3$ (hematite)] the following refinements of the sample preparation were performed: varying the La excess in order to compensate for La losses during the preparation process, checking the temperature range of stability with the available tubular furnace, reducing the heat treatment time and investigating different quenching methods.

The La hexaferrite samples with the lowest amount of secondary phases (see Table I) were for coprecipitation prepared with 50% La excess, heat treated at 1365 °C for 23 h, which contained 6% $LaFeO_3$ and 4% $Fe_2O_3$, and for mechanical alloying a pure sample with 2% La excess, heat treated at 1335 °C for 24 h. The presence of both, La rich and La depleted impurity phases in the coprecipitated (co.) $LaFe_{12}O_{19}$ indicates that the La excess for coprecipitation in this sample was near optimum (see phase diagram according to Ref. 10). The pure mechanical alloyed (MA) $LaFe_{12}O_{19}$ delivered a saturation magnetization of 74.7 $Am^2/kg$ at room temperature (in comparison SrM 74.3 $Am^2/kg$; see Ref. 2). All La hexaferrite samples exhibited a very small coercivity (in the order of 0.05 T) due to the large grain size of around 100 $\mu$m, as reported in Refs. 9 and 12. An attempt to reduce the grain size by milling failed, because of the metastability of the compound and resulted in a decomposition of the hexaferrite phase.

Partly La substituted Sr ferrite samples were prepared by coprecipitation as well as by mechanical alloying. Only one sample was prepared by coprecipitation (see Table I), following the same procedure as described above using in addition $Sr(NO_3)_2$ in a ratio of La/Sr=1/2.

For mechanical alloying the starting materials were oxides and carbonates. The samples were prepared according to the formula $(1-x)SrCO_3+\frac{x}{2}La_2(CO_3)_3+6Fe_2O_3$, using different La concentrations $x$. No La excess was used for these samples. The pure Sr ferrite was heat treated only for 2 h at 1000 °C, which is sufficient to form this phase. Table I shows the amount of secondary phases of these samples, determined by XRD, with the quantitative analysis performed by using the Rietveld method. All samples with concentrations higher than $x=0.2$, except $x=1$, contain a small amount of hematite ($Fe_2O_3$).

### B. Characterization of the samples

For phase analysis of the samples x-ray diffraction was performed at a Siemens D500 powder diffractometer with a graphite monochromator. Co $K\alpha$ radiation ($\lambda=1.79$ Å) at 35 mA and 30 kV was used. For low temperature diffraction a helium flow temperature controller down to 4.2 K was available. The evaluation of the data was performed with the software Topas by Bruker. For quantitative analysis the Rietveld method was employed.

Temperature dependent neutron diffraction experiments were performed at the Institute Laue Langevin, Grenoble, France, using the powder diffractometers D20 in its high takeoff option ($\lambda=1.887$ Å). The high resolution powder diffractometer D2B ($\lambda=1.594$ Å) was additionally employed in order to check for any possible symmetry changes. The Rietveld method using the FULLPROF program was used for the refinement of the neutron powder diffraction data.[13]

In order to observe phase transitions, the specific heat of La hexaferrite was measured in a quasiadiabatic calorimeter employing the step-heating method (for details see Ref. 14). A magnet and a He flow cryostat were available for field and temperature dependent measurements.

For measurements of magnetization and magnetocrystalline anisotropy a pulsed field magnetometer with a magnet for fields up to 30 T, a He flow cryostat for low temperature measurements and pulse durations of 10 and 1 ms was employed. The signal of the sample was detected with a coaxial pick-up system and integrated digitally. For anisotropy measurements the SPD method[15] was used, performing the second derivative of the magnetization signal with an analog differentiator.

ac susceptibility was measured with a Lake Shore ac susceptometer 7000. A He flow cryostat, a heater and a tempera-

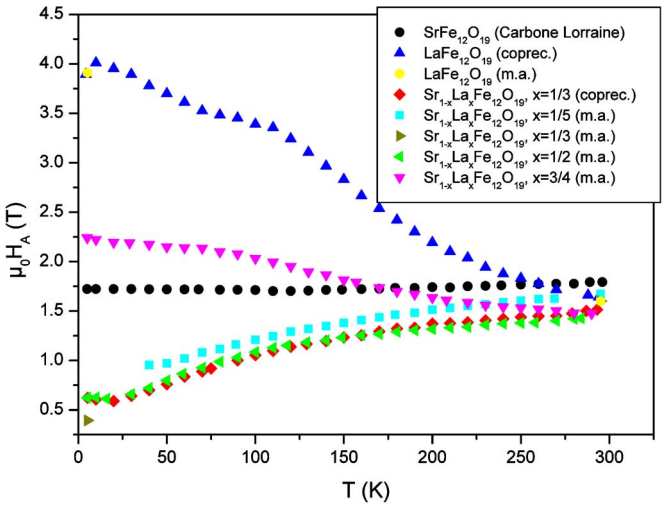


FIG. 1. (Color online) Anisotropy field versus temperature of La-substituted Sr hexaferrite with various concentrations, prepared by different methods.

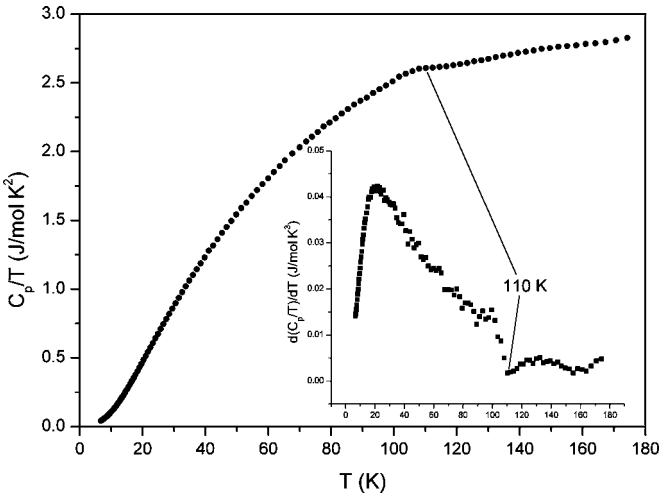


FIG. 2. $C_p/T$ versus $T$ of $LaFe_{12}O_{19}$ (co.); a hump at approximately 110 K is visible indicating a phase transition.

ture controller are used for temperature dependent measurements.

In order to observe the local environment of the Fe ions in the sample Mössbauer spectra of $^{57}Fe$ were obtained with a spectrometer using a $^{57}Co$ source in Rh matrix. For low temperature measurements a He flow cryostat with temperature controller was used, while for high temperature a furnace with temperatures up to 800 °C and a PID regulator was available.

The NMR spectra are envelopes of the Fourier transformed spin echos measured in a homemade phase coherent pulse spectrometer tuned at various frequencies and in zero applied field. The excitation conditions (typical pulse duration 3 $\mu$s, distance 40 $\mu$s) were optimized for the domain signal. The contributions from domain walls were small, as seen from measurements in the magnetically saturated state in fields up to 7 T along the easy axis of the aligned powders. Measurements in external fields were taken to identify spin up and down sites in the ferrimagnetic structure.

## III. RESULTS AND DISCUSSION

### A. La hexaferrite

According to an early publication on La hexaferrite[8] the most significant changes in comparison to conventional hexaferrites occur in the magnetocrystalline anisotropy, which was at that time calculated from the demagnetization curves measured at low temperatures. Figure 1 shows a measurement of the temperature dependent anisotropy field of La hexaferrite (co.) in comparison with a commercial Sr hexaferrite and La substituted Sr hexaferrite with various La concentrations. The anisotropy exhibits a remarkable increase from 1.64 T at room temperature up to 4.01 T at 10 K. For the mechanical alloyed $LaFe_{12}O_{19}$ only the values at room temperature and 4.2 K are shown and they match with the ones of the coprecipitated $LaFe_{12}O_{19}$.

This is in agreement with Lotgering,[8] who reported a value of around 40 kOe for the anisotropy field at 4.2 K. The increase was explained by the change from $Fe^{3+}$ to $Fe^{2+}$ at one of the lattice sites, in order to compensate the additional charge due to a valence difference of the $La^{3+}$ ion and the $Sr^{2+}$ ion. This results on one hand in a change of magnetization and, on the other hand, in a contribution to the anisotropy constant $K_1$ because of the orbital momentum of $Fe^{2+}$. From magnetization measurements it is known that the $Fe^{2+}$ ion is located on a spin up lattice site since the total moment is reduced by $1\mu_B$/formula unit. Assuming a preference of $Fe^{2+}$ for a site with octahedral coordination to account for the positive $K_1$ contribution Lotgering proposed the $2a$ site.

Remarkable in the measurement of anisotropy field of the La hexaferrite is a change in the slope at around 110 K. This indicates a magnetic or structural phase transition. Therefore the sample was further examined in a calorimeter and a susceptometer, in order to determine specific heat and susceptibility versus temperature.

The occurence of a phase transition is indeed confirmed by the specific heat results revealing a small hump at around 110 K (see Fig. 2). This feature appears as a symmetric anomaly, which is shown in the differentiated signal, where a curve similar to the derivative of a Gauss function occurs. It resembles a jump in $dC_p/T/dT$ but is not distinct enough to classify the phase transition. The maximum in the derivative near 20 K is the inflection point of the Debye function.

In the susceptibility signal of the La hexaferrite a change of slope at around 110 K is visible in the real part as well as a local maximum in the imaginary part (see Fig. 3). Above this transition the imaginary part is very small, reversible processes seem to dominate and hysteresis losses are small. Interesting is a second local maximum in $\chi''$ at around 35 K that does neither appear in $\chi'$ nor in the specific heat. This could indicate a magnetic transition without structural transition, although they usually go together in ferrites, since the Fe spins are strongly coupled to the lattice. A further indication of such a transition at low temperature might be the change of slope observed in the anisotropy field at low temperature (see Fig. 1). For future experiments temperature dependent hysteresis loop measurements of magnetically aligned samples are planned.

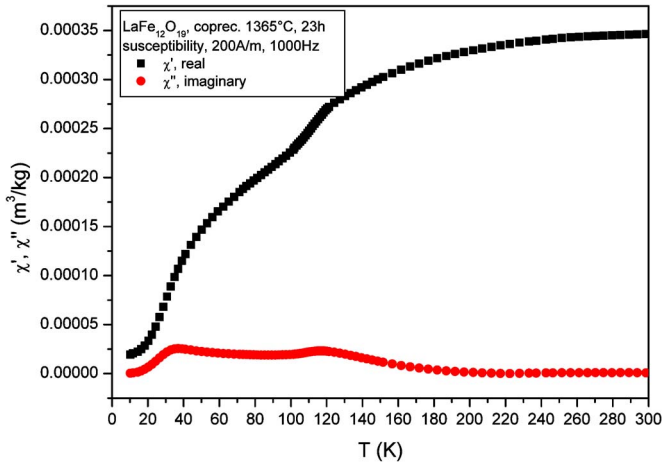


FIG. 3. (Color online) Real and imaginary part of $\chi$ versus $T$ of $LaFe_{12}O_{19}$ (co.); a hump at approximately 110 K is visible indicating a phase transition.

A confirmation of a structural phase transition occurring below room temperature was found in the x-ray diffractograms. A careful comparison between the diffractograms at room temperature and at 4.2 K revealed a distortion of the hexagonal crystal lattice to an orthorhombic structure with space group *Cmcm*. The distortion is evident in the splitting of the peak $hkl=(2\,2\,0)$ in the $P6_3/mmc$ structure in two peaks corresponding to $hkl=(4\,0\,0)$ and $hkl=(2\,6\,0)$ at 4.2 K (see Fig. 4). This splitting was also found for the peak of lower order, $hkl=(1\,1\,0)$, although here the peak shows only a shoulder at the left, since the resolution is worse at smaller angles. This splitting indicates a distortion in the basal plane of the hexagonal structure. Since the (4 0 0) peak was shifted to lower angles, which corresponds to an increased lattice plane distance, the parameter $a$ is elongated in the distorted structure, while the (2 6 0) peak is shifted to higher angles, so that $b$ must be shortened (see also neutron diffraction Table II). From the line shift a distortion of the order $\Delta d/d = 1\%$ was calculated. The sixfold symmetry of the (2 2 0) planes is broken in a twofold symmetry for the (4 0 0) planes and a fourfold symmetry for the (2 6 0) planes. The intensity ratio of the peaks in the x-ray pattern corresponds usually to the symmetry and indeed the (2 6 0) peak exhibits an intensity approximately two times as high as for the (4 0 0) peak (see Fig. 4).

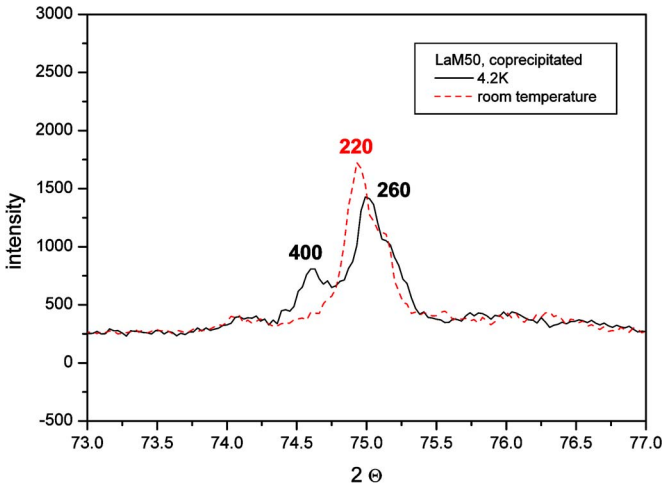


FIG. 4. (Color online) Splitting of the (2 2 0) peak of $LaFe_{12}O_{19}$ (co.) at 4.2 K; the splitting is characteristic for a distortion to an orthorhombic structure.

TABLE II. Lattice parameters of La hexaferrite from neutron diffraction at room temperature and at 4.2 K ($\lambda = 1.594$ Å).

| temperature | $a$ [Å] | $b$ [Å] | $c$ [Å] |
|---|---|---|---|
| 295 K | 5.8858 (1) | 10.1944 (2) | 22.8887 (4) |
| 4.2 K | 5.9025 (1) | 10.1593 (2) | 22.7883 (4) |

A clear signature of the structural transition was also found in the thermodiffractogram of the neutron diffraction experiments performed at ILL Grenoble. Figure 5 shows a detail of a temperature scan from 295 K down to 10 K with wave length 1.887 Å. A splitting of the peaks (4 1 4) at 119.6° and (4 0 11) at 120.5° occurs at temperatures lower than 101 K, which indicates a temperature induced change of the crystal structure. The lattice parameters were obtained from the high resolution measurement at room temperature and at 4.2 K and are shown in Table II. An orthorhombic description was used for the hexagonal lattice with $b=a\sqrt{3}$. Compared with typical values for Sr hexaferrite [$a=b=5.883$ Å and $c=23.037$ Å (Ref. 16)] the parameters $a$, $b$ are slightly increased while $c$ is reduced. The distorted lattice has a doubled unit cell (see Fig. 6) and the five Fe sites change in the Wyckoff notation from $2a$, $2b$, $4f1$, $4f2$, $12k$ to $4a$, $4c$, $8f1$, $8f2$, $8f3$, and $16h$, so that $12k$ is split in two sites. The assignment of the sites in the different spacegroups is not trivial and was observed with NMR measurements. The atom positions of the two different crystal structures obtained from a Rietveld refinement of the high resolution neutron diffraction data at room temperature and 4.2 K are shown in Table III.

Figure 7 shows a comparison of the $^{57}$Fe NMR spectrum of $LaFe_{12}O_{19}$ (MA) with that of a conventional Sr hexaferrite (without the $2b$-Fe line at 59.7 MHz) measured at 4.2 K. At 4.2 K La hexaferrite is in the orthorhombic distorted phase. The site assignment for the Sr hexaferrite is well known

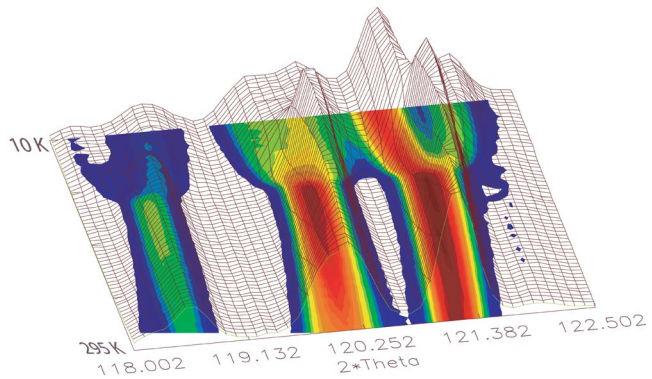


FIG. 5. (Color online) Splitting of peaks in the neutron diffractogram of $LaFe_{12}O_{19}$ at low temperature indicating a structural phase transition.

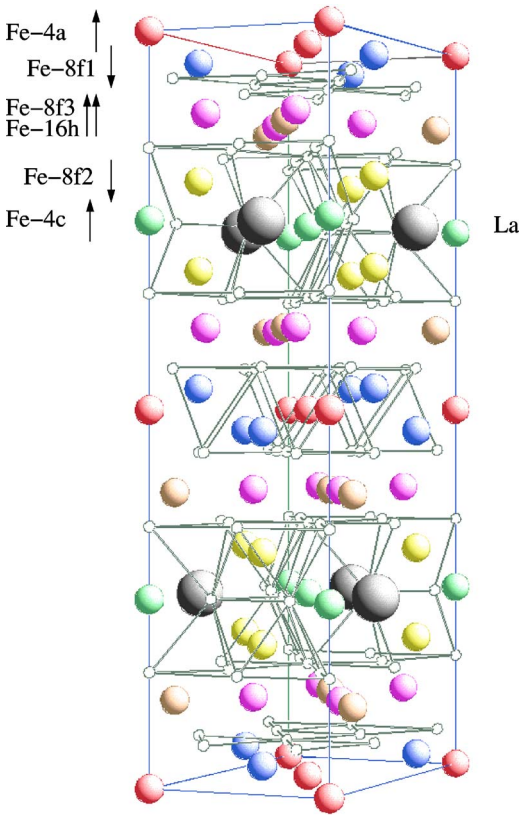


FIG. 6. (Color online) Distorted crystal lattice of the La hexaferrite with orthorhombic *Cmcm* spacegroup. The 12*k* site splits in the 16*h* and 8*f*3 sites.

from the literature. The sites corresponding to (anti)parallel moments in the orthorhombic structure were identified by application of an external field along the easy axis of the powder, and from the changes in the spectra with La concentration (see below).

First of all it is seen that the signal from 4*a*-Fe in La hexaferrite is missing. It was not possible to obtain a spin echo from this site at any temperature down to 1.3 K, and with pulse distances down to 10 $\mu$s, even though the resonance frequency (41.8 MHz) is known to within a few hundred kHz from Mössbauer spectroscopy (see below). This is ascribed to the different time scales of the measurements: NMR is very sensitive to slow fluctuations of the hyperfine field which induce fast relaxation of the nuclear magnetization and can, thereby, prevent the formation of an observable spin echo at pulse distances available in this experiment. The same holds for the 2*b* site which can be measured in Sr hexaferrite, but which could not be detected near 61.5 MHz in the orthorhombic structure.

As for the other Fe sites it is seen that both 4*f*1 and 4*f*2 are shifted to smaller hyperfine fields ($f=B_{\mathrm{hf}}/\gamma$, where $f$ is the resonance frequency, $B_{\mathrm{hf}}$ the field at the nucleus, and $\gamma=1.3757$ MHz/T) in the distorted structure. A shift to higher hyperfine fields can be seen for the 16*h* line of the La hexaferrite when comparing it to the 12*k* line of the Sr hexaferrite phase. Note that the line assigned to the 16*h* site contains only 2/3 of the relative intensity of the 12*k* line when compared with the 4*f*1 site, clearly showing the splitting of

TABLE III. Atom positions in the two different lattice structures of La hexaferrite determined from neutron diffraction at $\lambda=1.594$ Å.

| atom | Wyckoff | *x* | *y* | *z* |
|---|---|---|---|---|
| | 295 K | $P6_3/mmc$ | | |
| La | 2*d* | 1/3 | 2/3 | 3/4 |
| Fe | 12*k* | 0.1671 (4) | 0.3342 (4) | −0.1089(1) |
| Fe | 4*f*1 | 1/3 | 2/3 | 0.1888 (1) |
| Fe | 4*f*2 | 1/3 | 2/3 | 0.0277 (2) |
| Fe | 2*b* | 0 | 0 | 1/4 |
| Fe | 2*a* | 0 | 0 | 0 |
| O | 12*k* | 0.5076 (8) | 0.0153 (8) | 0.1544 (1) |
| O | 12*k* | 0.1583 (8) | 0.3166 (8) | 0.0550 (2) |
| O | 6*h* | 0.1841 (10) | 0.3682 (10) | 1/4 |
| O | 4*f* | 1/3 | 2/3 | −0.0558(3) |
| O | 4*e* | 0 | 0 | 0.1536 (2) |
| | 4.2 K | *Cmcm* | | |
| La | 4*c* | 0 | 0.3388 (18) | 1/4 |
| Fe | 16*h* | 0.2500 (8) | 0.0835 (4) | 0.8915 (2) |
| Fe | 8*f*1 | 0 | 0.1689 (5) | 0.1092 (3) |
| Fe | 8*f*2 | 0 | 0.3316 (6) | 0.6890 (1) |
| Fe | 8*f*3 | 0 | 0.3332 (7) | 0.5280 (2) |
| Fe | 4*b* | 0 | −0.0016(9) | 1/4 |
| Fe | 4*a* | 0 | 0 | 0 |
| O | 16*h* | 0.2340 (10) | 0.2547 (7) | 0.1555 (2) |
| O | 16*h* | 0.2351 (11) | 0.0812 (7) | 0.0557 (3) |
| O | 8*f*1 | 0 | 0.1605 (9) | 0.5554 (5) |
| O | 8*f*2 | 0 | 0.4934 (9) | 0.1547 (4) |
| O | 8*f*3 | 0 | 0.3372 (11) | 0.0565 (3) |
| O | 8*g* | 0.2793 (14) | 0.0848 (10) | 1/4 |
| O | 8*f*4 | 0 | 0.0005 (15) | 0.1542 (2) |
| O | 4*c* | 0 | 0.8192 (12) | 1/4 |

(2)12*k* into 16*h* and 8*f*3 sites. The signal from the 8*f*3 site is ascribed to the broad shoulder down to 70.5 MHz, where it is difficult to separate from signals with large turning angles which might also originate from 8*f*1 domain wall signals. This assignment is supported by Mössbauer spectroscopy which cannot resolve the splittings in this part of the spectrum but which shows clearly that the hyperfine fields of all the 12*k* sites remain in this part of the spectrum in the distorted structure.

From Fig. 8 it is seen that with increasing temperature the line of 16*h*-Fe develops an additional, unresolved splitting. In addition all three sites (8*f*2 not shown) shift to slightly higher frequency with increasing temperature. The origin of this behavior is not clear up to now but most likely it is connected with the low temperature maximum in the imaginary part of the susceptibility and with the change in slope of the anisotropy field mentioned above. The shift to higher local fields is unusual since $B_{\mathrm{hf}}$ is in good approximation proportional to the sublattice magnetization which is ex-

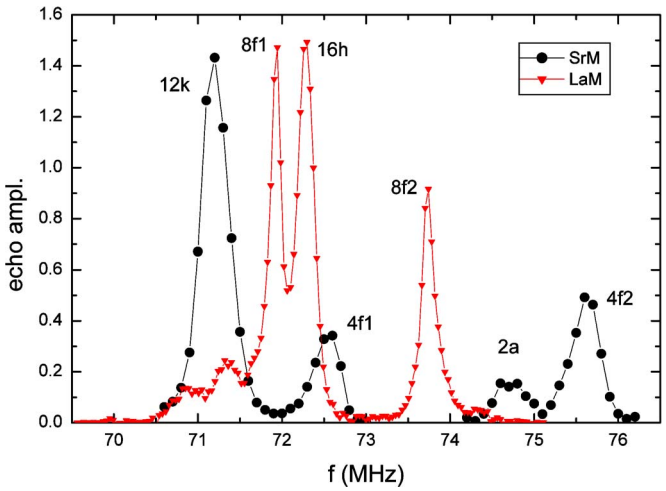


FIG. 7. (Color online) Pointwise Fourier transformed NMR spectrum of $LaFe_{12}O_{19}$ (MA) in comparison with that of a commercial Sr ferrite (sintered) measured at 4.2 K.

pected to decrease with increasing temperature. The splitting might be due to the 16*h* sites separating into two magnetically inequivalent sites with the local differing by app. 0.15 T. Since there is no additional splitting from magnetic symmetry in a collinear ferrimagnetic structure this might indicate a slightly canted magnetic structure at temperatures above 10 K. Another indication of a magnetic low temperature instability is the fact that the relaxation rates increase steeply with temperature, so it was not possible to detect any spin echo above 35 K, the temperature of the susceptibility maximum.

While the resolution of Mössbauer spectroscopy is insufficient to detect the low temperature magnetic transition it does not suffer from the relaxation time problems of NMR and shows clear indications of the structural transition at 100 K. In Fig. 9 (see also Table IV) the spectra of La hexaferrite at room temperature and 4.2 K are shown. From the decomposition of the spectrum of the hexagonal structure (room temperature) into the five sites it is seen that the hyperfine field at all sites increases with decreasing tempera-

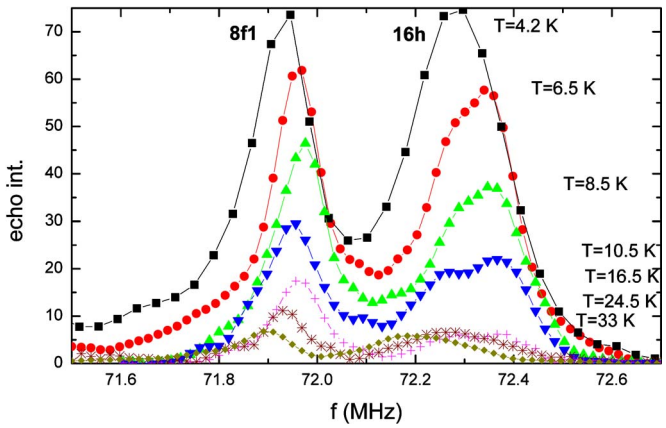


FIG. 8. (Color online) Temperature dependence of the line assigned to the 16*h* site in the NMR spectrum of $LaFe_{12}O_{19}$ (MA); the line shows a splitting at higher temperatures.

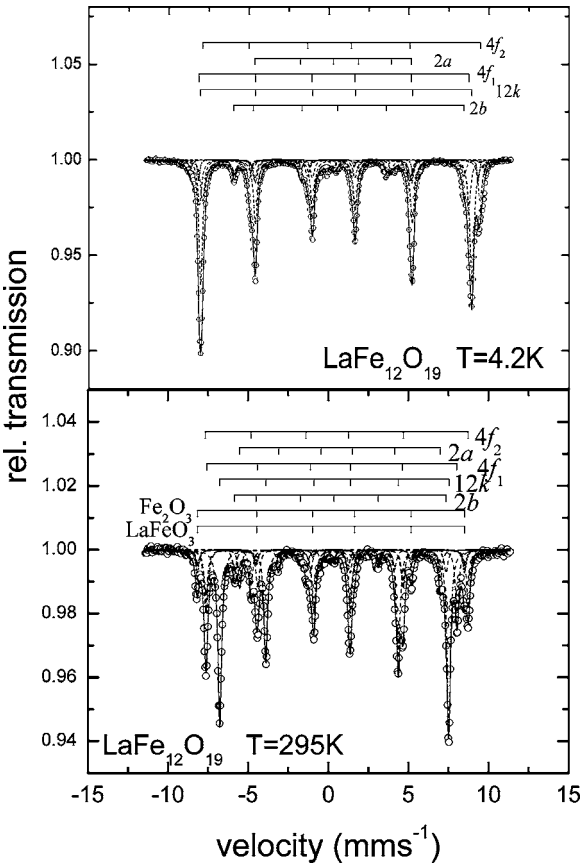


FIG. 9. Comparison of the Mössbauer spectra of $LaFe_{12}O_{19}$ (co.; including impurities $LaFeO_3$ and $Fe_2O_3$) at room temperature and 4.2 K.

ture, except the one for the 2*a* site, which *decreases* dramatically from 38 to 30 T. The quadrupole splitting of all sites remains the same, again with the exception of 2*a*-Fe, where the component of the electric field gradient along the local magnetic field changes from practically zero to a negative value (−0.8 mm/s) nearly half as large as the (positive) one of the 2*b* site; the isomer shift is large (0.65 mm/s) only for the 2*a* site. It depends on temperature for the 2*a* and 2*b* sites but stays constant for the others.

This behavior will be discussed in the context of band structure calculations in a separate publication but may qualitatively be understood as follows: the quadrupole shift at room temperature is small for all sites except the bipyramidal 2*b*-Fe because the electric field gradient vanishes (almost) in the nearly cubic oxygen coordinations. In the orthorhombic distorted structure at low temperature this near cubic symmetry is lost at the 4*a* site, resulting in a sizeable electric field gradient. The large isomer shift of 2*a*-Fe is a clear indication that this site is occupied by $Fe^{2+}$, localizing the electron doped into the structure by the substitution of $Sr^{2+}$ with $La^{3+}$. This is in contrast to the findings in our earlier study of the calculated hexaferrite (room temperature) band structure, where no indication of any localization of the doped electron was found.[17] Since localization does occur in new calculations of the orthorhombic structure this is most probably due to the fact that in the former calculations the structural transition was not considered and, therefore, did

TABLE IV. Hyperfine fields, quadrupole shift, and isomer shift of the five Fe sublattices in La hexaferrite at 4.2 K and room temperature taken from Mössbauer measurements.

| | Fe site | $T=295$ K | $T=4.2$ K |
|---|---|---|---|
| $B_{HF}$ [T] | 12*k* | 43.86 | 52.67 |
| $B_{HF}$ [T] | 4*f*1 | 48.01 | 52.32 |
| $B_{HF}$ [T] | 4*f*2 | 50.55 | 53.91 |
| $B_{HF}$ [T] | 2*b* | 40.58 | 44.67 |
| $B_{HF}$ [T] | 2*a* | 38.45 | 30.38 |
| Quad. [mm/s] | 12*k* | 0.19 | 0.1 |
| Quad. [mm/s] | 4*f*1 | 0.15 | 0.04 |
| Quad. [mm/s] | 4*f*2 | 0.66 | 0.33 |
| Quad. [mm/s] | 2*b* | 1.47 | 0.93 |
| Quad. [mm/s] | 2*a* | 0.34 | 0.23 |
| Iso. [mm/s] | 12*k* | 0.28 | 0.23 |
| Iso. [mm/s] | 4*f*1 | 0.16 | 0.16 |
| Iso. [mm/s] | 4*f*2 | 0.22 | 0.27 |
| Iso. [mm/s] | 2*b* | 0.02 | 0.23 |
| Iso. [mm/s] | 2*a* | 0.59 | 0.7 |

not allow for any structural relaxation upon La substitution in the earlier calculations. Finally, the increase of the hyperfine field with decreasing temperature corresponds to the increase of the sublattice magnetization. The drastic reduction at the 4*a* site is attributed to an unquenched orbital momentum at $Fe^{2+}$. The orbital momentum induces a hyperfine field which is opposite the one from the spin moments, leading to a partial cancellation.

A further confirmation for the localization of the additional electron at the 2*a* site at room temperature was found in the high resolution neutron diffractogram. Table V shows the magnetic moments observed at the different Fe lattice sites in four different experiments: (a) high resolution experiment at the D2B spectrometer using a wavelength of 1.4 Å; (b) experiment at the D20 spectrometer with wavelength 1.6 Å and a 10 in. collimator; (c) experiment at the D20 spectrometer with wavelength 1.6 Å using full flux and only the central part of the detector; (d) experiment at the D20 spectrometer with wavelength 1.6 Å using full flux and the full height of the detector. A reduction of the magnetic moment is visible at the 2*a* site, which indicates in agreement with the Mössbauer measurements the formation of $Fe^{2+}$. The magnetic moment is for all sites much lower than $5\mu_B$ as for the free $Fe^{3+}$ ion, because a significant part is transferred to the oxygen ions, and a part of electrons is in the interstitial region, which is in agreement with the conductivity of the sample at room temperature. Another reason is that the measurement was performed at room temperature, where the magnetization is approximately 10% lower than at 0 K.

TABLE V. Magnetic moments at room temperature at the different Fe sites determined by neutron diffraction; (a) D20, 1.4 Å; (b) D2B, 1.6 Å, 10 in. coll.; (c) D2B, 1.6 Å, Fullflux1; (d) D2B, 1.6 Å, Fullflux2.

| Fe site | (a) $\mu_B$ | (b) $\mu_B$ | (c) $\mu_B$ | (d) $\mu_B$ |
|---|---|---|---|---|
| 12*k* | 3.6 | 3.8 | 3.8 | 3.7 |
| 4*f*2 | 3.8 | 3.7 | 4.0 | 4.1 |
| 4*f*1 | 3.8 | 3.9 | 3.9 | 3.7 |
| 2*b* | 3.5 | 3.9 | 4.0 | 3.9 |
| 2*a* | 3.4 | 3.4 | 3.5 | 3.1 |

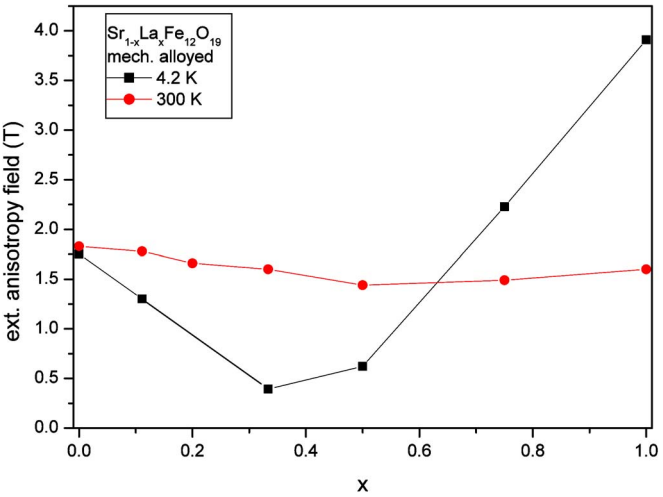


FIG. 10. (Color online) Anisotropy field versus La concentration *x* at 4.2 K and at room temperature.

### B. La substituted Sr hexaferrite

For the partly with La substituted Sr hexaferrite samples the anisotropy shows completely different behaviors (see Fig. 1). Only the sample with $x=0.75$ shows the same tendence as the pure La ferrite, but a less strong increase in anisotropy. Again a change in slope is visible, for this sample at around 90 K. For the sample with $x=0.2$ only values down to 40 K are shown. Below this temperature the SPD peak vanishes, which may indicate an inhomogeneous change from uniaxial to planar anisotropy. The samples $x=0.33$, coprecipitated, and $x=0.5$, mechanical alloyed, are almost indistinguishable. While for the Sr hexaferrite ($x=0$) the anisotropy is almost constant and for a La concentration of $x=0.75$ the anisotropy field increases as in the La hexaferrite, for all other La concentrations it *decreases* with decreasing temperature.

Figure 10 shows a clear dependence of the magnetocrystalline anisotropy measured at room temperature and at 4.2 K on the La concentration. At room temperature the anisotropy is decreasing almost linearly by 21% at $x=0.5$ and then increasing slightly up to a value of 1.6 T for the La ferrite (Sr ferrite: 1.83 T). There is some uncertainty in comparing the values, due to the demagnetizing field. It was not possible to cut the brittle samples in exactly the same way, so that the demagnetizing field of the slightly different geometries may differ a few percent. At 4.2 K again the anisotropy

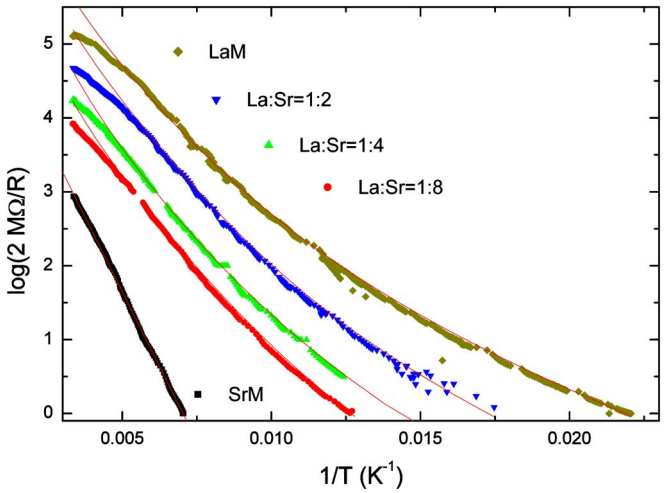


FIG. 11. (Color online) Resistance from room temperature down to 30 K of Sr ferrites substituted with different La concentrations, measured on pressed powder pellets during cooling (see text for the fitted lines).

decreases, but only up to $x=0.33$, and increases then rapidly to reach a value of 3.9 T for the pure La ferrite. From this one can see that the anisotropy decreases with decreasing temperature for $x=0$ to $x=0.5$ and increases at La concentrations higher than $x\approx 0.6$, where both curves cross. This is rather astonishing, since in all the partly substituted samples some kind of charge compensation has to take place when substituting $Sr^{2+}$ by $La^{3+}$ and this finding indicates that this mechanism might change with concentration.

The charge compensation can take place in a delocalized state by incomplete filling of a band as was indicated by earlier band structure calculations,[17] by the formation of polarons, as discussed in Ref. 18 for the case of small La concentrations,[23,24] or in form of a localized $Fe^{2+}$ ion. The large and temperature dependant change in the magnetic anisotropy clearly indicates a single-ion contribution and, thereby, localization of the electrons at one of the Fe sites, at least at low temperatures.

Localization is also supported by measurements of the electrical resistance. Figure 11 shows the electrical resistance of La-substituted Sr ferrite samples prepared by mechanical alloying. The samples were pressed to cylindrical pellets with a cross section of 1 $cm^2$ and a height of $2.9\pm0.05$ mm. Since all samples have the same dimensions a comparison of the resistance is possible. A specific resistivity or a conductivity is not given, since the porosity of the samples, grain boundary influence, impurities and defects in the structure are undetermined. Furthermore, the measurements especially at intermediate La concentrations exhibited some hysteresis between cooling and heating which cannot totally be attributed to incomplete thermalization of the bulky samples since the room temperature resistance also changed significantly (up to 20%). The resistance measurement was performed in zero magnetic field from room temperature down to app. 30 K with 2 MΩ as an upper limit within the experimental setup.

The room temperature resistance is changing with increasing La concentration from 2.3 kΩ for pure Sr hexaferrite to 16 Ω for pure La hexaferrite. At small La concentrations the temperature dependence below room temperature can be described by a simple semiconducting behavior with the energy gap of app. 3700 K for Sr hexaferrite dropping continuously to app. 2100 K (0.18 eV) for $LaFe_{12}O_{19}$ (lines in the figure). The value of 0.35 eV for the ceramic Sr hexaferrite is significantly lower than the one for crystalline $BaFe_{12}O_{19}$ given in the literature [0.8 eV (Ref. 19)] and might indicate some nonintrinsic behavior. The curvature of the data between room temperature and approximately 150 K especially at higher doping indicates that the effective gap in these samples is too small to allow a consistent description in terms of a nondegenerate semiconductor up to room temperature. The semiconductor characteristics changes to a much smaller temperature dependance at low $T$ for all doped samples, indicating that another transport mechanism takes over when the conductivity of the semiconducting regions becomes too small. The fit to the low temperature resistivity of the La hexaferrite shows that $R(T)$ can be described virtually over the whole temperature region by a stretched exponential (even more at intermediate $x$). The value $n=1/4$ chosen for the exponent has been associated with variable range hopping,[20] as have been values up to $n=1/2$, which describe the data as well. Thus, the whole resistance curve can be described by a parallel circuit of a semiconductor and a material exhibiting a variable range hopping characteristic (lines at intermediate $x$). These behaviors might be associated with the grains and grain boundaries, respectively, which are present in all samples. It is noteworthy that there is no indication of the structural phase transition in any of the resistance measurements.

For none of the partly substituted samples a structural phase transition was observed in the neutron diffraction pattern, including the one with $x=0.75$, although it exhibits a change in slope in the anisotropy similar to La hexaferrite. A careful Rietveld analysis was performed and delivered a good fit assuming the hexagonal crystal structure for all samples at room temperature as well as at 4.2 K. Figure 12 shows the change in the lattice parameter $a$ and $c$ determined by x-ray diffraction at room temperature. An increase of only 0.2% from $x=0$ to $x=1$ ($x\cdots$La concentration) occurs in the parameter $a$, but it is not linear in the concentration and exhibits a bigger slope at higher concentrations. While parameter $a$ increases with the La concentration, the lattice parameter $c$ decreases. This decrease is stronger than the increase in $a$ so that the unit cell volume decreases, too (see also Fig. 12). For the volume a linear fit is more suitable, according to the Vegard law.[21,22] The value $x=1$ is an outlier and one of the possible explanations could be the difference in preparation, since the starting materials were here solely oxides, while for the partly substituted samples La and Sr carbonate were used. Table VI gives an overview of the values.

If the reasoning of Lotgering was true, the additional electron from La doping will only enter the $2a$ site, where it always enhances the anisotropy. The fact that the anisotropy *decreases* with La concentration up to $x=0.5$ strongly indicates that the electron is localized first at or near another site where it either induces a negative $K_1$ contribution or at least suppresses positive contributions to the anisotropy.

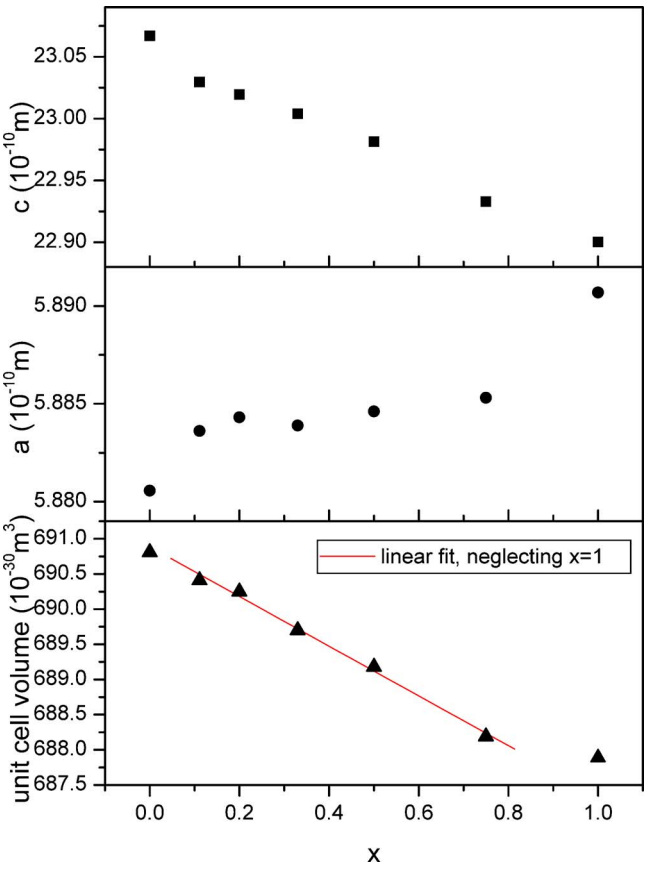


FIG. 12. (Color online) Change in lattice parameter $a$ and $c$ and in unit cell volume with the nominal La concentration $x$; all samples were prepared by mechanical alloying and XRD was performed at room temperature; errors are smaller than the symbol size.

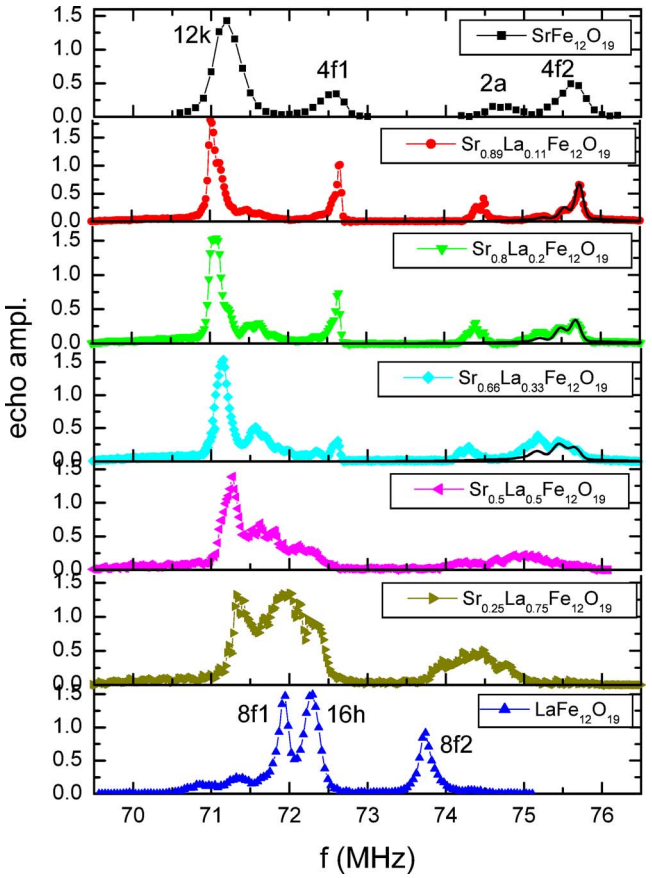


FIG. 13. (Color online) NMR spectra of La substituted Sr hexaferrite with various La concentrations, prepared by mechanical alloying, in comparison with that of a commercial Sr ferrite (sintered).

Figure 13 shows zero field NMR spectra of all samples prepared by mechanical alloying with different La concentrations. At the small concentration La/Sr=1/8 the spectrum resembles the one of pure SrM. The comparatively broad lines of the pure Sr hexaferrite may be attributed to the fact that this sample is a commercial powder with grain size in the single domain regime where a higher defect concentration might be expected (and are, in fact, intended to provide pinning centers for domain walls). All four peaks of the sites 12$k$, 4$f$1, 2$a$, and 4$f$2 are present, but at all sites resolved or unresolved satellite lines and some line broadening occur. This is in clear contrast to earlier findings in La doped Sr hexaferrite where at $x$=0.1 all lines shifted without developing satellites.[18] The reason is unclear but the different preparation process might induce other defect structures or, as mentioned above, the La concentration in the samples studied there could be significantly smaller than the nominal one. The satellites are due to different local environments of the Fe ions, caused by the substitution. By measuring in an external field the satellites were assigned to the main peaks, showing increasing (spin down sites 4$f$1 and 4$f$2), or decreasing (spin up sites 2$a$ and 12$k$) local field with increasing applied field.

TABLE VI. Comparison of the lattice parameters a and c of mechanical alloyed samples at room temperature; $x_{nom}$ is the nominal La concentration according to the starting materials; $vol_{UC}$ is the volume per unit cell; sec. ph. is the amount of secondary phase in the sample, in this case $Fe_2O_3$.

| compound | $x_{nom}$ | $a=b$ [$10^{-10}$ m] | $c$ [$10^{-10}$ m] | $vol_{UC}$ [$10^{-30}$ m$^3$] | sec. ph. [%] |
|---|---|---|---|---|---|
| $SrFe_{12}O_{19}$ | 0 | 5.8806 | 23.0669 | 690.81 | 0 |
| $Sr_{0.88}La_{0.11}Fe_{12}O_{19}$ | 0.11 | 5.8836 | 23.0296 | 690.41 | 0 |
| $Sr_{0.8}La_{0.2}Fe_{12}O_{19}$ | 0.2 | 5.8843 | 23.0196 | 690.25 | 0 |
| $Sr_{0.66}La_{0.33}Fe_{12}O_{19}$ | 0.33 | 5.8839 | 23.0039 | 689.70 | 8 |
| $Sr_{0.5}La_{0.5}Fe_{12}O_{19}$ | 0.5 | 5.8846 | 22.9814 | 689.18 | 6 |
| $Sr_{0.25}La_{0.75}Fe_{12}O_{19}$ | 0.75 | 5.8853 | 22.9329 | 688.19 | 12 |
| $LaFe_{12}O_{19}$ | 1 | 5.8907 | 22.9003 | 687.89 | 0 |

Up to a La concentration of $x$=0.3 the effect on the 2$a$ and 12$k$ sites is comparatively small: Both show a broadening from unresolved satellites, and 12$k$ shifts slightly to higher frequency (local field) while the local field at 2$a$-Fe becomes smaller on average. There is no loss in relative intensity of the 2$a$ resonance that would be expected if this site would capture the additional electrons as it does in the fully substituted La hexaferrite discussed above. The initial effect of La doping is, in contrast, large on the 2$b$ site (not shown), as well as on 4$f$1 and 4$f$2 Fe: the 2$b$ resonance

broadens severely and shifts to 60.5 MHz at $x=0.2$, but it was impossible to detect the signal at higher concentrations. The $4f1$ and $4f2$ sites both develop resolved satellite lines which are especially for $4f1$ Fe relatively far from the main line ($\approx 1$ MHz or 0.7 T). Inspection of the crystal structure shows that this can easily be understood for $2b$ and $4f2$ Fe, which are nearest neighbors of Sr. La substitution on that site changes their environment significantly. The satellites of $4f2$ Fe at $x=0.11$ can be described reasonably well by assuming a binomial distribution for their intensities following the probability of up to all three nearest Sr neighbors being replaced by La (see lines in Fig. 13 for $x=0.11$, 0.2, and 0.33). At $x=0.2$ and 0.33 this underestimates the relative intensities of the satellites assigned to two and three La nearest neighbors. The effect is too large to be ascribed to a higher than nominal La concentration but could be due to a variation of the nuclear resonance enhancement factor if the local anisotropy decreases around a La ion. The $4f1$ sites are, on the other hand, neighbors of $2a$-Fe and far from the Sr site. The strong influence of La doping on this site supports, therefore, the assumption that the decreasing single-ion contributions to the magnetic anisotropy at small $x$ have their origin in the localization of the doped electrons near the tetrahedral $4f1$ sites. On the other hand, the local field changes by less than 2%, much less than the local moment and, thereby, the local field are expected to change if this satellite would correspond to $Fe^{2+}$ on a $4f1$ site. This indicates that localization takes place not directly at but near this site, which is in accord with the general rule that there is simply not enough space for the large $Fe^{2+}$-ion in a tetrahedral configuration.

The spectra also show in agreement with the diffraction data that there is no structural phase transition down to 4.2 K, at least for concentrations up to $x=0.5$. However, at this concentration several changes in the shape of the spectra indicate that at least locally the structural distortion corresponding to the orthorhombic structure takes place: The $2a$ site vanishes, intensity piles up in the frequency range of the $8f1$ and $16h$ sites of the *Cmcm* structure, and the broad $4f2$ resonance shifts rapidly to the lower local fields of the $8f2$ site in the orthorhombic structure. This suggests that there is a concentration threshold near $x=0.5$ above which the charge compensation switches from the $4f1$ to the $2a$ site.

## IV. CONCLUSION

The obtained x-ray and neutron diffraction data show that the lattice parameter $c$ decreases with increasing La concentration, while $a$ is increasing slightly. The unit cell volume therefore decreases linearly with increasing La concentration. The most interesting result was that the pure La hexaferrite exhibits a lattice distortion near $T=100$ K. This distortion takes place mainly in the basal plane of the hexagonal lattice, increasing the parameter $a$ but reducing $b$ in the orthorhombic description. The structure can be described by the spacegroup *Cmcm*. The distortion was observed in the thermodiffractogram obtained by neutrons, the signature of the phase transition was found in the specific heat, as well as in the ac susceptibility. A change of structure was not observed any of the partly La-substituted Sr ferrite samples. However, the NMR spectra indicate the presence of the corresponding local distortions at concentrations higher than $x=0.5$.

An early study has reported a remarkably high magnetic anisotropy of $LaFe_{12}O_{19}$ at low temperature and suggested that this is due to an unquenched orbital momentum of $Fe^{2+}$ on the $2a$ site. It was shown here that the anisotropy field is, in fact, increasing continuously from room temperature to 4.0 T at 4.2 K, with a clear change in slope at the structural phase transition. From the isomer shift in the Mössbauer spectra it is evident that charge compensation indeed takes place at $2a$ Fe at room temperature as well as at 4.2 K in the orthorhombic structure. The same indication was found in the magnetic moment of the five different Fe sublattices, observed by neutron diffraction. The hyperfine field at the $2a$ site strongly supports the view that the large temperature dependent single-ion contribution to the anisotropy from this site depends on the size of the orbital momentum as well as on changes in the crystal field induced by the structural transition. The details of this model will be compared to band structure calculations in a separate publication.

From the studies of samples at intermediate La concentrations evidence was found for the existence of a concentration threshold at $x\approx 0.5$, where the Fe site responsible for the charge compensation appears to change. For samples with lower concentration the magnetic anisotropy decreases with decreasing temperature and the NMR spectra show a relatively strong influence of the La doping on the $4f1$ site. In contrast, the magnetic anisotropy field increases with decreasing temperature for higher concentrations, and simultaneously the $2a$ resonance vanishes from the NMR spectrum which regroups to resemble the one of the pure La hexaferrite.

The experience with preparing $LaFe_{12}O_{19}$ leads to the conclusion that the metastability of the compound at room temperature makes it difficult to exploit the large low temperature anisotropy of this material in technical applications. Nevertheless, by systematic studies of the intricate relationship between structure, orbital momentum and magnetic anisotropy a better understanding may be obtained of how these technically important parameters are changed by substitution.

## ACKNOWLEDGMENTS

This work was supported by the Austrian Science Foundation under Grant Nos. P15700-N02, P16500-N02, and by the EU project ALFA AML/B7-311/97/0666II-0147-FI.

*Electronic address: kuepfer@ifp.tuwien.ac.at

[1] J. J. Went, G. W. Ratheneau, E. W. Gorter, and G. W. VanDosterhout, Philips Tech. Rev. **13**, 194 (1951).
[2] H. Kojima, *Ferromagnetic Materials* (North-Holland, Amsterdam, 1982), Vol. 3.
[3] A. G. Smolenski and A. A. Andreev, Bull. Acad. Sci. 25, 1405 (1961).
[4] K. Iida, Y. Minachi, K. Masuzawa, M. Kawakami, H. Nishio, and H. Taguchi, J. Phys. Soc. Jpn. **23**, 1093 (1999).
[5] J. F. Wang, C. B. Ponton, and I. R. Harris, J. Magn. Magn. Mater. **234**, 233 (2001).
[6] J. F. Wang, C. B. Ponton, and I. R. Harris, IEEE Trans. Magn. **38**, 2928 (2002).
[7] J. F. Wang, C. B. Ponton, R. Grössinger, and I. R. Harris, J. Alloys Compd. **369**, 170 (2004).
[8] F. K. Lotgering, J. Phys. Chem. Solids **35**, 1633 (1974).
[9] M. Küpferling, V. Corral-Flores, R. Grössinger, and J. Matutes-Aquino, J. Magn. Magn. Mater. **290-291**, 1255 (2005).
[10] V. L. Moruzzi and M. W. Shafer, J. Am. Ceram. Soc. **43**, 367 (1960).
[11] J. Ding, D. Maurice, W. F. Miao, P. G. McCormick, and R. Street, J. Magn. Magn. Mater. **150**, 417 (1995).
[12] M. Küpferling, R. Grössinger, M. W. Pieper, G. Wiesinger, and M. Reissner, IEEE Trans. Magn. (to be published).
[13] J. Rodriguez-Carvajal, Physica B **192**, 55 (1993).
[14] S. Manalo, H. Michor, M. El-Hagary, G. Hilscher, and E. Schachinger, Phys. Rev. B **63**, 104508 (2001).
[15] G. Asti and S. Rinaldi, Phys. Rev. Lett. **28**, 1584 (1972).
[16] K. Kimura, M. Ohgaki, K. Tanaka, H. Morikawa, and F. Marumo, J. Solid State Chem. **87**, 186 (1990).
[17] P. Novák, K. Knížek, M. Küpferling, R. Grössinger, and M. W. Pieper, Eur. Phys. J. B **43**, 509 (2005).
[18] M. W. Pieper, M. Küpferling, I. R. Harris, and J. F. Wang, J. Magn. Magn. Mater. **272-276**, 2219 (2004).
[19] J. Smit and H. P. J. Wijn, *Ferrites* (Gloeilampenfabrieken, Eindhoven, 1959).
[20] N. F. Mott and E. A. Davis, *Electronic Processes in Noncrystalline Materials* (Clarendon, Oxford, 1979).
[21] L. Vegard, Z. Phys. **5**, 17 (1921).
[22] L. Vegard, Z. Kristallogr. **67**, 148 (1928).
[23] L. Lechevallier, J. M. LeBreton, J. F. Wang, and I. R. Harris, J. Magn. Magn. Mater. **269**, 192 (2004).
[24] The samples studied there were prepared via a nonstandard hydrothermal route. There are indications that the actual rare earth concentration within the hexaferrite structure at least above $x=0.2$ is significantly smaller than the nominal concentration given there (see also Ref. 23).